

Nonlinear bubble dynamics of cavitation

Yu An

Department of Physics, Tsinghua University, Beijing 100084, China

(Received 13 October 2011; published 9 January 2012)

For cavitation clouds generated in a standing sound wave driven by an ultrasonic horn, the nonlinear acoustic wave equation governing cavitation dynamics is numerically solved together with the bubble motion equation under an approximation. This conceptual calculation can qualitatively reproduce the observed characteristics of cavitation.

DOI: [10.1103/PhysRevE.85.016305](https://doi.org/10.1103/PhysRevE.85.016305)

PACS number(s): 47.35.Rs, 43.35.Ei, 43.25.Yw, 43.30.Nb

I. INTRODUCTION

Acoustic cavitation is a complicated phenomenon. In liquid, some individual micron-sized gas bubbles generated by an intense ultrasonic wave assemble to form luminescent gas bubble clouds [1,2]. Driven by the intense acoustic wave, every bubble vibrates violently by expanding with the negative sound pressure phase and rapidly contracting with the positive sound pressure phase and rebounding. These vibrating bubbles produce acoustic radiation pressure and become sources of sound waves. When a bubble is compressed to its minimum size, its very high internal temperature and pressure cause it to flash. The study of single-bubble vibration in addition to the interaction between bubbles may achieve a good understanding of cavitation phenomena [3]. Unfortunately, this solution is very difficult for practical use. We have to count on the nonlinear sound wave equation in bubbly liquid to study cavitation dynamics [4]. In the present paper, we recur to a theoretical framework for studying cavitation dynamics. It consists of a nonlinear sound wave equation in an acoustic cavitation environment together with the bubble radial

motion equation. Under an appropriate approximation, we numerically solve the equations and compare the calculation to observation.

II. THEORY AND FORMULAS

The bubbles interact with each other through the radiation pressure. For any time t and any place \vec{r} , the radiation pressure contributed by the cavitation bubbles [5] is

$$p_{\text{int}}(\vec{r}, t) = \rho_l \sum_j \frac{[2R_j(t')\dot{R}_j^2(t') + R_j^2(t')\ddot{R}_j(t')]|_{t'=t-\frac{|\vec{r}-\vec{r}_j|}{c_l}}}{|\vec{r} - \vec{r}_j|}, \quad (1)$$

where $R_j(t)$ is the radius of the j th bubble placed at \vec{r}_j , ρ_l is the liquid density, and c_l is the sound speed in the liquid at ambient temperature and pressure (1 atm). Equation (1) is only valid for $|\vec{r} - \vec{r}_j| \gg R_j(t)$, which is equivalent to a dilute bubble distribution. If the bubble number density is assumed to be $N(\vec{r}, t)$, then the right terms in Eq. (1) may be approximately expressed as the integral

$$p_{\text{int}}(\vec{r}, t) = \rho_l \int \frac{N(\vec{r}', t')[2R(\vec{r}', t')\dot{R}^2(\vec{r}', t') + R^2(\vec{r}', t')\ddot{R}(\vec{r}', t')]|_{t'=t-\frac{|\vec{r}-\vec{r}'|}{c_l}}}{|\vec{r} - \vec{r}'|} dV'. \quad (2)$$

We can make the analogy $p_{\text{int}} \rightarrow$ electric potential and $\rho_l N(2R\dot{R}^2 + R^2\ddot{R}) \rightarrow$ electric charge density. Then, referring to the electromagnetic equation, we find that the expression (2) is the solution to the equation

$$\nabla^2 p_{\text{int}} - \frac{1}{c_l^2} \frac{\partial^2 p_{\text{int}}}{\partial t^2} = -4\pi\rho_l N(2R\dot{R}^2 + R^2\ddot{R}). \quad (3)$$

If there is no cavitation, the sound wave equation is

$$\nabla^2 p - \frac{1}{c_l^2} \frac{\partial^2 p}{\partial t^2} = 0. \quad (4)$$

Combining Eqs. (3) and (4), the acoustic wave equation in the cavitation environment may be expressed as

$$\nabla^2 p - \frac{1}{c_l^2} \frac{\partial^2 p}{\partial t^2} = -4\pi\rho_l N(2R\dot{R}^2 + R^2\ddot{R}), \quad (5)$$

where p is the total acoustic wave pressure. Equation (5) was derived earlier with the equations of fluid mechanics

under sound wave approximation [6]. Usually, there are many different kinds of bubbles in the cloud, so we may sort the number density of the bubble with the ambient radius $R_{0i}(\vec{r}, t)$ as $N_i(\vec{r}, t)$ and the bubble radius $R_i(\vec{r}, t)$. Then, Eq. (5) turns to

$$\nabla^2 p - \frac{1}{c_l^2} \frac{\partial^2 p}{\partial t^2} = -4\pi\rho_l \sum_i N_i(2R_i\dot{R}_i^2 + R_i^2\ddot{R}_i). \quad (6)$$

To solve Eq. (6) we need to know $R_i(\vec{r}, t)$. In an acoustic cavitation environment, bubbles usually move slowly [2]. Then, the i th bubble vibration equation should be [7,8]

$$\begin{aligned} (1 - M_i)R_i\ddot{R}_i + \frac{3}{2}\left(1 - \frac{M_i}{3}\right)\dot{R}_i^2 \\ = (1 + M_i)\frac{1}{\rho_l}[p_{li} - p_\infty - p_{si}(t + t_{R_i})] + \frac{t_{R_i}}{\rho_l}\dot{p}_{li} - \frac{p_{\text{int}}}{\rho_l}, \end{aligned} \quad (7)$$

where p_∞ is the ambient pressure, $p_{si}(t)$ is the driving acoustic pressure at the i th bubble, ω is the angular frequency of the sound wave, $t_{R_i} \equiv R_i/c_l$, $p_{li} = p_{gi}(R_i, t) - 4\eta\dot{R}_i/R_i - 2\sigma/R_i$ is the pressure on the liquid side of the i th bubble wall, $p_{gi}(R, t)$ is the pressure on the gas side of the i th bubble wall, η is the shear viscosity, and σ is the surface tension coefficient of the liquid. $M_i \equiv \dot{R}_i/c_l$ is the bubble-wall Mach number. In the present work, we focus on the bubble dynamic processes. This allows us to use an isothermal approximation in the calculation (i.e., assume the pressure inside a bubble to be $p_g = \frac{\mu\bar{R}T}{V-b} + p_v$, where μ is the gas mole number, \bar{R} is the gas constant, V is the bubble volume, b is the van der Waals hard core volume, and p_v is the vapor pressure of the surrounding liquid). For the case of $M_i = 0$ in Eq. (7), since $t_{R_i} \sim 0$, we have

$$R_i \ddot{R}_i + \frac{3}{2} \dot{R}_i^2 = \frac{p_{li} - p}{\rho_l} + \frac{t_{R_i}}{\rho_l} \dot{p}_{li}, \quad (8)$$

where $p = p_\infty + p_{si}(t) + p_{\text{int}}$ is the total acoustic pressure in Eq. (6). On the other hand, Eqs. (7) and (8) are only valid for $M_i \ll 1$. With the analogy of Eq. (7), we may expect a slightly modified form of bubble pulsation equation to the first order of M_i is

$$(1 - M_i)R_i \ddot{R}_i + \frac{3}{2} \left(1 - \frac{M_i}{3}\right) \dot{R}_i^2 = (1 + M_i) \frac{p_{li} - p}{\rho_l} + \frac{t_{R_i}}{\rho_l} \dot{p}_{li}. \quad (9)$$

Thus, the sound wave in the cavitation environment is governed by Eqs. (6) and (9). For a few simple cases, such as a small bubble cluster or bubble filament, the radiation pressure may be approximately calculated by Eq. (1) [8,9]. In most other cases, however, we have to solve Eqs. (6) and (9), which are not only more fundamental but also more practical.

III. NUMERICAL RESULTS AND DISCUSSIONS

Let us consider a case with a cylindrical ultrasonic horn as the source of sound waves with its tip immersed in water contained in a cylindrical flask. Suppose the diameter of the flask is 8 cm, the water column is 16-cm high, and the horn diameter is 1 cm. The tip of the horn dips 2 cm into the top center surface of the water. The sound pressure is input sinusoidally at the horn tip surface $p_s = -p_a \sin \omega t$. In our case, the frequency is set to 20 kHz. Since N_i is unknown, we have to make an approximation to solve Eqs. (6) and (9). We assume that only one kind of bubble forms cavitation clouds, that the ambient radius $R_{0i} = R_0$ for all bubbles, and we typically set $R_0 = 4.5 \mu\text{m}$. These bubbles are homogeneously distributed in the cavitation clouds and do not move. We also assume there are no bubbles outside the clouds. These assumptions simplify Eq. (6) to Eq. (5) and allow us to ignore the subscript i in Eq. (9). This approximation may seem too simple to be realistic. However, when the calculated results are compared to observation, the main physics seems preserved in the approximation.

For highly degassed water at 20°C, suppose the amplitude of the driving acoustic pressure $p_a = 2.5 \text{ atm}$ is not intense enough to induce cavitation. Then, solving Eq. (4), we obtain a standing sound wave. In the calculation, we use cylindrical coordinates with the downward z axis coinciding with the

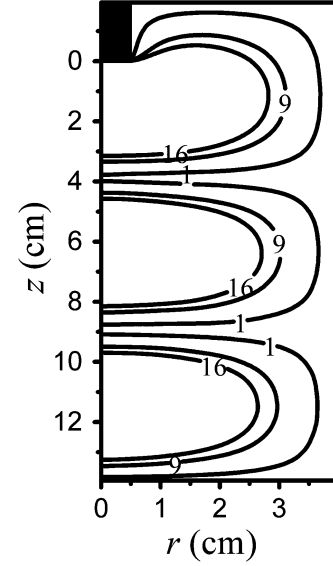


FIG. 1. Contour of the relative intensity of sound wave for $p_a = 2.5 \text{ atm}$ in water in the absence of cavitation. The black block is the horn.

symmetric axis of the flask, and the horn tip surface is set at $z = 0$. If we focus on the axially symmetric solutions (axially asymmetric solutions are possible for a nonlinear system), the problem may be simplified to two dimensions. To describe the sound wave field, the relative intensity of sound wave at any time t and any place \vec{r} is set as $I(\vec{r}, t) = 2 \int_t^{t+T} [p(\vec{r}, t')/p_\infty - 1]^2 dt'/T$, where T is the period of the driving acoustic wave. Figure 1 shows the distribution of the relative intensity at a vibrating period.

For less degassed water, $p_a = 2.5 \text{ atm}$ usually causes cavitation when the number density of bubble N relates to the sound pressure p in a very complicated way. In our calculation, we simply let N rely on the calculated sound pressure when

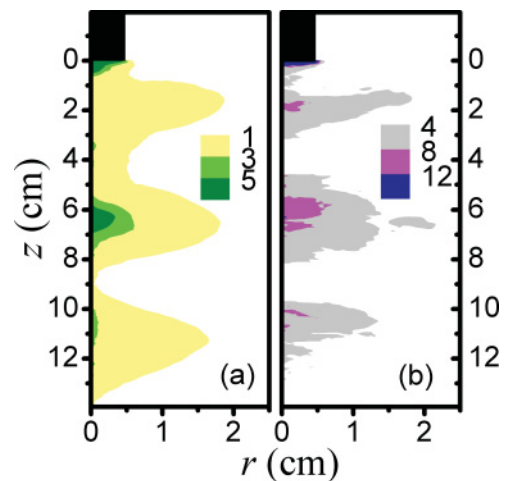


FIG. 2. (Color online) (a) Color-fill (grayscale) contour of the relative intensity of sound wave in water for $p_a = 2.5 \text{ atm}$, $N = 1.0 \times 10^9 \text{ m}^{-3}$. (b) Color-fill (grayscale) contour of R_M/R_0 . The black block is the horn.

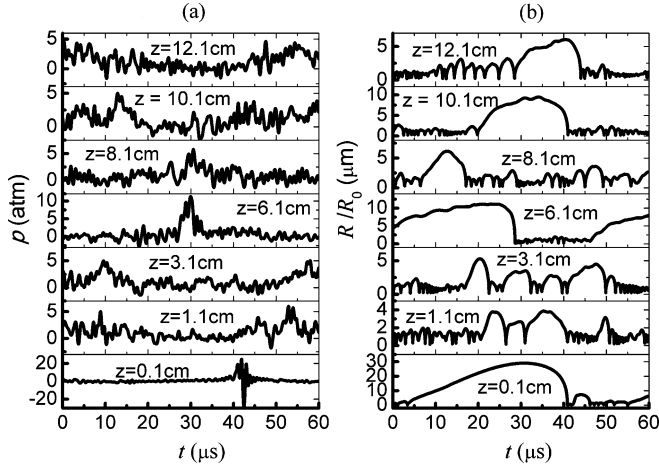


FIG. 3. For the case of Fig. 2, (a) the acoustic pressure p and (b) R/R_0 at different places on the axis ($r = 0$) as a function of time.

cavitation is ignored. We assume that bubbles survive when the amplitude of sound pressure without cavitation is larger than 1.0 atm, and the bubble density N is set to be nonzero, which in Fig. 1 corresponds to the region with a relative intensity larger than 1.0. Suppose $N = 1.0 \times 10^9 \text{ m}^{-3}$ (the average distance between bubbles is 1 mm). Then, we can numerically solve Eqs. (5) and (9) (ignoring the subscript i). Figure 2(a) shows that the relative intensity of the sound wave is suppressed by cavitation, specifically in the high-intensity region, compared to Fig. 1. Such a standing acoustic wave drives every bubble in the cavitation clouds, which disturbs the sound wave in return. The violent extent of the bubble motion is usually related to the ratio of the maximum bubble radius to the ambient radius (i.e., R_M/R_0) and is also related to the brightness of the bubble. In water, if $R_M/R_0 < 8$, the bubble is too dim to observe its flash, and if $R_M/R_0 > 12$, the bubble is bright. Figure 2(b) shows that the vicinity of the horn tip surface is the only area where lightening bubbles are observed. For more details of the sound

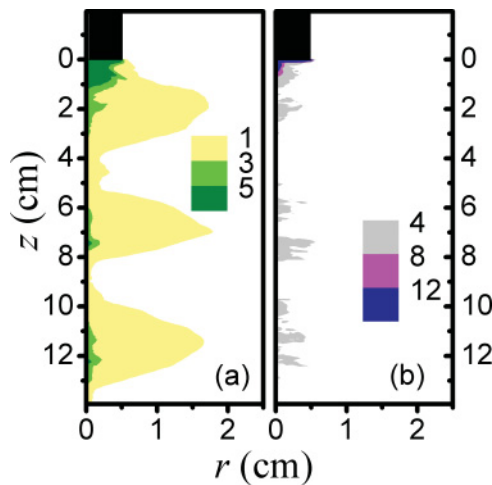


FIG. 4. (Color online) (a) Color-fill (grayscale) contour of the relative intensity of sound wave in water for $p_a = 2.5$ atm, $N = 5.0 \times 10^9 \text{ m}^{-3}$. (b) Color-fill (grayscale) contour of R_M/R_0 . The black block is the horn.

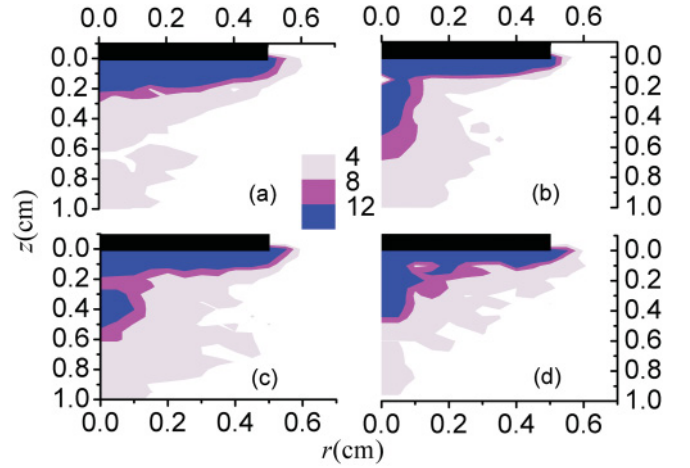


FIG. 5. (Color online) Color-fill (grayscale) contour of R_M/R_0 in vicinity of the horn (black blocks) tip surface in water, for the cases (a) $p_a = 2.5$ atm, $N = 1.0 \times 10^9 \text{ m}^{-3}$, (b) $p_a = 2.5$ atm, $N = 5.0 \times 10^9 \text{ m}^{-3}$, (c) $p_a = 3.0$ atm, $N = 5.0 \times 10^9 \text{ m}^{-3}$, and (d) $p_a = 3.5$ atm, $N = 5.0 \times 10^{10} \text{ m}^{-3}$.

wave and the bubble motion, we plot the acoustic pressure p , in Fig. 3(a), and the ratio of the bubble radius to its ambient radius R/R_0 , in Fig. 3(b), at different points of the axis ($r = 0$) as functions of time. Though the driving signal is purely sinusoidal, the sound wave in the cavitation environment is seriously distorted. The curve profile of R/R_0 as a function of time is also very different from the single-bubble case except for a bubble in the vicinity of the horn tip surface. We also find that the times at which a bubble is compressed to its minimum size are different for bubbles at different places (i.e., bubbles in different places flash at different times).

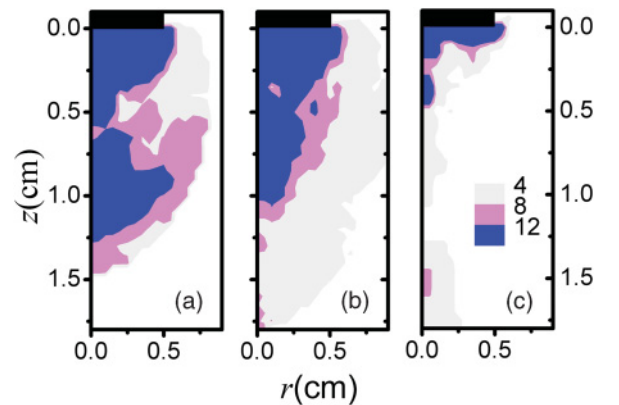


FIG. 6. (Color online) Color-fill (grayscale) contour of R_M/R_0 in vicinity of the horn (black block) tip surface in strong sulfuric acid, in the cases (a) $p_a = 4.0$ atm, $N = 1.0 \times 10^9 \text{ m}^{-3}$, (b) $p_a = 5.0$ atm, $N = 2.0 \times 10^9 \text{ m}^{-3}$, and (c) $p_a = 6.0$ atm, $N = 5.0 \times 10^{10} \text{ m}^{-3}$. The sulfuric acid column is 10-cm high, and the horn dips 2.5 cm into the top center surface of the sulfuric acid. The parameters for strong sulfuric acid used in the calculation are as follows: the density is 1778.6 kg/m^3 , the sound speed is 1000 m/s , the surface tension coefficient is 0.0681 N/m and the shear viscosity is 0.0237 N s/m^2 . Other conditions are the same as in water.

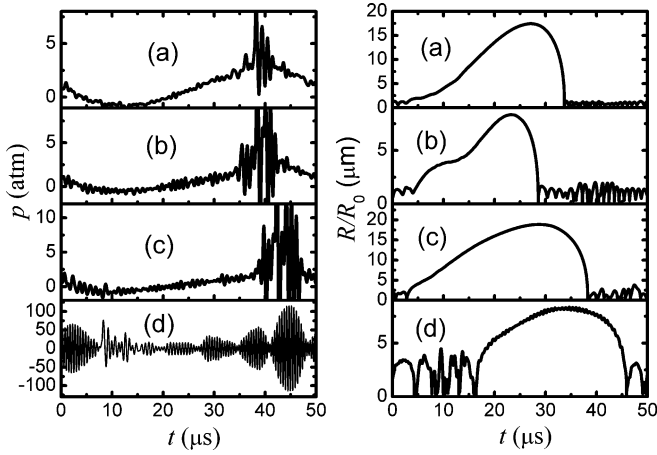


FIG. 7. Acoustic pressure p (left) and R/R_0 (right) at $r = 0.45$ cm and $z = 0.1$ cm as functions of time. (a)–(d) correspond to the same cases as in Fig. 5.

If the gas concentration in water is higher, there are more cavitation bubbles. Suppose $N = 5.0 \times 10^9 \text{ m}^{-3}$. Comparing Fig. 4 to Fig. 2 ($N = 1.0 \times 10^9 \text{ m}^{-3}$), we see that the sound wave intensity weakens a little but the violent extent of the bubble motion is dramatically decreased, which shows that the input power is spread by a larger number of bubbles. We may roughly investigate how the light emission of bubbles depends on the bubble density in the cavitation clouds and the input intensity of the driving acoustic wave. Figure 5 shows the contour of R_M/R_0 in the vicinity of the horn tip surface for various p_a and N . It is apparent that the bubble density N suppresses the lightening area in the cavitation cloud. Since N increases with p_a , a simple increase of the input power may not always favor the luminosity of a cavitation cloud. A similar phenomenon occurs in strong sulfuric acid as well. Figure 6 shows the contour of R_M/R_0 in the vicinity of the horn tip surface for three different p_a and N in strong sulfuric acid at 20°C . Since R_M/R_0 roughly reflects the luminosity of the bubble, Fig. 6 may be thought to be qualitatively consistent with observation [2]. To further understand how the sound pressure and the bubble radius at the light-emitting region change with time and how they behave with varying p_a and

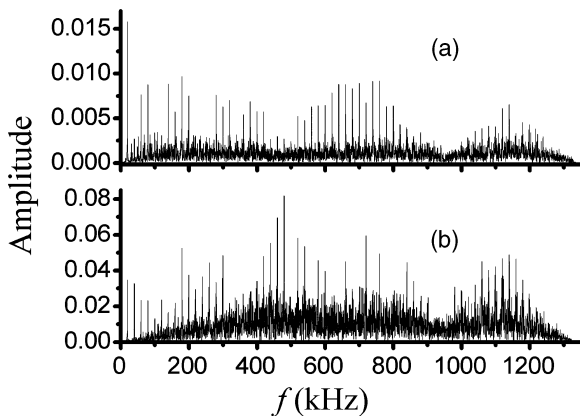


FIG. 8. Power spectral density of sound pressure in water for the case of Fig. 2. (a) at P : $r = 3.95$ cm, $z = 6$ cm, (b) at Q : $r = 0$, $z = 13.95$ cm.

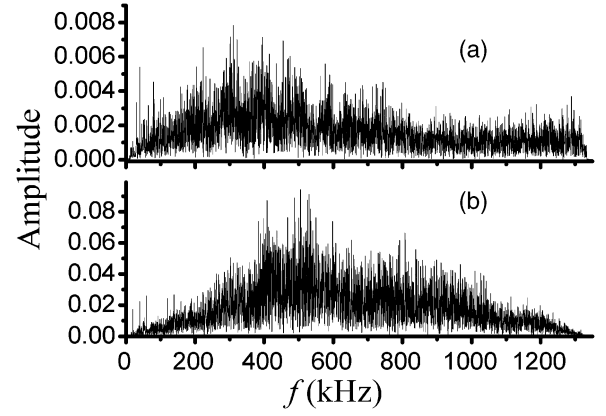


FIG. 9. Power spectral density of sound pressure in water for the case of Fig. 5(d). (a) at P : $r = 3.95$ cm, $z = 6$ cm, (b) at Q : $r = 0$, $z = 13.95$ cm.

N , Fig. 7 shows p and R/R_0 at $r = 0.45$ cm and $z = 0.1$ cm as functions of time for the cases in Fig. 5. We see that for $p_a = 3.5$ atm and $N = 5.0 \times 10^{10} \text{ m}^{-3}$ the sound wave is no longer sinusoidal at all, and R/R_0 represents symmetric profile, such a phenomenon was observed experimentally [10].

The analysis of the acoustic signal is an important mean in the experiment [11]. The next calculation provides the power density of the sound pressure calculated by Eq. (5). We choose two points in the sound wave field; the point P is at a lateral middle of the water, $r = 3.95$ cm and $z = 6$ cm, and the other point Q is at the bottom of the water, $r = 0$ and $z = 13.95$ cm. Figure 8(a) shows the power spectral density for the case in Fig. 2. We see prominent multiple-frequency components in the weak noise background, but the basic frequency is still dominant. Therefore, the acoustic pressure roughly retains good periodicity. However, at Q [see Fig. 8(b)], multiple-frequency components as well as noise are stronger at high frequency, which represents strong nonlinearity. In our calculation we also notice a cutoff frequency at ~ 1.33 MHz for those multiples and noises that is independent of R_0 , p_a , and N , but slightly depends on ω and the flask dimension. Occasionally, for $p_a = 2.0$ atm and $N = 2.0 \times 10^9 \text{ m}^{-3}$, we observe bifurcation at low frequency. If the input signal is stronger and there are more cavitation bubbles, both at P and Q those multiples emerge into the noise background and the sound pressure almost loses its periodicity and becomes chaotic (see Fig. 9). Since the equation is nonlinear, both bifurcation and chaos [11] are natural.

IV. CONCLUSION

The nonlinear sound wave equation together with the bubble pulsation equation may describe cavitation dynamics. However, this theoretical framework does not include a method of determining the parameters N_i , which was simply set to be some possible values in the numerical trials. Therefore, the calculation is only conceptual, not simulative. Determining the optimum N_i is finding the equation of state of the cavitation cloud, which is an open problem. Furthermore, though the bubbles move slowly in cavitation clouds and their direct effect on the sound wave may be negligible, their motion affects

N_i . We cannot yet determine whether this indirect effect is negligible. However, the main physics is indeed included in Eqs. (6) and (9), which can correctly describe the dynamics of cavitation in our approximate calculation.

ACKNOWLEDGMENTS

The author deeply appreciates valuable discussion with Dr. K. Yasui. Project No. 10974116 was supported by the NSFC.

-
- [1] K. R. Weninger, C. G. Camara, and S. J. Putterman, *Phys. Rev. E* **63**, 016310 (2000).
 - [2] H. Xu, N. C. Eddingsaas, and K. S. Suslick, *J. Am. Chem. Soc.* **131**, 6060 (2009).
 - [3] K. Yasui, T. Tuziuti, J. Lee, T. Kozuka, A. Towata, and Y. Iida, *Ultrason. Sonochem.* **17**, 460 (2010).
 - [4] C. Vanhille and C. Campos-Pozuelo, *Ultrasound in Med. and Biol.* **34**, 792 (2008).
 - [5] R. Löfstedt, B. P. Barber, and S. J. Putterman, *Phys. Fluids A* **5**, 2911 (1993).
 - [6] E. A. Zabolotskaya and S. I. Soluyan, *Sov. Phys. Acoust.* **18**, 396 (1973).
 - [7] J. B. Keller and M. Miksis, *J. Acoust. Soc. Am.* **68**, 628 (1980).
 - [8] Y. An, *Phys. Rev. E* **83**, 066313 (2011).
 - [9] K. Yasui, Y. Iida, T. Tuziuti, T. Kozuka, and A. Towata, *Phys. Rev. E* **77**, 016609 (2008).
 - [10] T. Tuziuti *et al.*, *Ultrason. Sonochem.* **12**, 73 (2005).
 - [11] C. D. Ohl, T. Kurz, R. Geisler, O. Lindau, and W. Lauterborn, *Philos. Trans. R. Soc. London A* **357**, 269 (1999).